Acta Mechanica Solida Sinica (2025) 38:25–32
https://doi.org/10.1007/s10338-024-00530-3

FULL-LENGTH ARTICLE

Enhancement of Quality Factor in Gain-Assisted Acoustic Resonance Systems

Lei Zhang[1] · Linlin Geng[1] · Yonghui Zhang[1] · Youdong Duan[1] · Jinbo Yuan[1] · Xiaoming Zhou[1]

Received: 7 April 2024 / Revised: 26 August 2024 / Accepted: 3 September 2024 / Published online: 21 October 2024

Abstract
Damped acoustic systems have a limited quality factor due to intrinsic loss. By introducing gain elements, a method to enhance the quality factor of damped systems is proposed based on the concept of bound states in the continuum (BICs). The acoustic model under study is a two-port waveguide system installed with two side Helmholtz resonators connected by a coupling tube. Based on the temporal coupled-mode theory, a Hamiltonian matrix with both intrinsic and radiation losses is used to characterize the resonance behavior of the coupled resonators. To achieve a high quality factor, acoustic gain is introduced to compensate the intrinsic loss, leading the Hamiltonian parameters toward a quasi-BIC condition. Numerical simulation demonstrates a gain-assisted and quasi-BIC-supported extremely high quality factor in damped acoustic systems. The concept is further utilized to design a sensor model for particle size detection. The enhanced sensing performance due to high quality factors is numerically demonstrated. The findings suggest potential applications in acoustic sensing and detection devices.

Keywords Acoustic resonance · Quality factor · Bound states in the continuum · Coupled-mode theory

1 Introduction

The quality factor is an important parameter describing the resonance behavior of oscillator systems [1]. The resonance with a high quality factor is highly demanded in acoustic sensing [2–4], filtering [5, 6], and detection devices [7, 8]. For a realistic system, the quality factor Q is affected by intrinsic energy damping and radiation loss. While inherent damping is usually unavoidable, radiation loss, which characterizes energy leakage from the resonator to the exterior environment, can be minimized through proper system designs. Recent efforts have been devoted to the suppression of radiation loss based on the concept of bound states in the continuum (BICs) in order to achieve high quality factors [9–12]. BICs are trapped modes residing in the continuum spectrum, and can provide zero radiation to the outside environment. There are different working mechanisms for forming acoustic localized modes, including symmetry-protected BICs [13–15], accidental BICs [16–18], Fabry-Perot BICs [19–21], and Friedrich-Wintgen BICs [22–26]. Quasi-BICs, which are modified pure BICs with slight radiation, can interact with the external environment and achieve an extremely high quality factor in systems with weak intrinsic damping.

In acoustic resonators, viscous damping can significantly weaken the resonance behavior, especially in the presence of small apertures. Even if radiation loss is diminished, inherent damping can still constrain the quality factor of acoustic resonance. To overcome this limitation, the gain element can be introduced into a damped system to compensate for energy dissipation. However, the design methods and high-Q performance of gain-assisted BIC systems remain underexplored. It is worth noting that BIC systems exhibit non-Hermitian characteristics. Over the past decade, non-Hermitian acoustics has witnessed a rapid development [27–29], leveraging the unique properties of balanced gain and loss. The relevant study can provide guidance for the design of acoustic gain elements. For example, acoustic gain can be realized in a loudspeaker system shunted with negative resistance circuits to construct a non-Hermitian exceptional point [30]. The loudspeaker structure can be equivalently represented by an impedance boundary condition, where acoustic gain is created by negative resistance effect.

✉ Xiaoming Zhou
zhxming@bit.edu.cn

[1] Key Laboratory of Dynamics and Control of Flight Vehicle of Ministry of Education, School of Aerospace Engineering, Beijing Institute of Technology, Beijing 100081, China

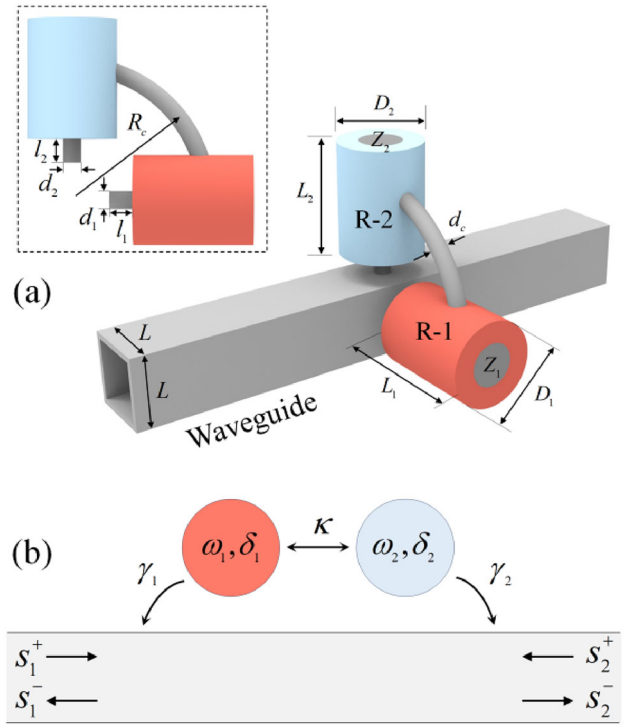

Fig. 1 **a** Schematic illustration of acoustic coupled-resonator system. A straight hollow waveguide of side length L is connected to two Helmholtz resonators with the diameter $D_{1,2}$ and height $L_{1,2}$. The cylindrical neck of the resonator has the diameter d_i and height l_i. Two resonators are connected by an annular tube of diameter d_c and distance R_c. Acoustic impedance boundary $Z_{1,2}$ used to produce energy gain occupies a circular area of diameter $D_{1,2}/2$. **b** The coupled-mode model of acoustic system in (**a**)

In this work, the enhancement of the quality factor in a two-port waveguide system with coupled resonators is studied. In the presence of air viscous damping, acoustic gain is introduced into the system in terms of the impedance boundary with negative resistances to compensate for energy dissipation. Based on the temporal coupled-mode theory, the gain–loss balance and quasi-BICs are simultaneously attained in damped acoustic systems, leading to high-Q performance. A sensor model for particle size detection is designed to demonstrate the advantages of the proposed high-Q acoustic system.

2 Model and Theory

The acoustic model under study consists of a straight rectangular waveguide coupled to a pair of Helmholtz resonators, which are connected by an annular tube, as shown in Fig. 1. Let the modal amplitudes of the two resonators be denoted by a_1 and a_2. In the waveguide, s_1^+ and s_2^+ represent the complex amplitudes of input waves incident from the left and right sides, respectively, while s_1^- and s_2^- stand for those of outgoing waves. Based on the temporal coupled-mode theory [31], the dynamic equations for this two-port coupled-resonator system are governed by

$$\begin{cases} -i\dfrac{\mathrm{d}\boldsymbol{a}}{\mathrm{d}t} = \boldsymbol{H}\boldsymbol{a} + \boldsymbol{K}^{\mathrm{T}}\boldsymbol{s}^{+} \\ \boldsymbol{s}^{-} = \boldsymbol{C}\boldsymbol{s}^{+} + \boldsymbol{D}\boldsymbol{a} \end{cases} \tag{1}$$

with

$$\boldsymbol{H} = \begin{bmatrix} \omega_1 + i\delta_1 + i\gamma_1 & \kappa + i\sqrt{\gamma_1\gamma_2} \\ \kappa + i\sqrt{\gamma_1\gamma_2} & \omega_2 + i\delta_2 + i\gamma_2 \end{bmatrix} \tag{2}$$

$$\boldsymbol{C} = \begin{bmatrix} 0 & 1 \\ 1 & 0 \end{bmatrix}, \quad \boldsymbol{K} = \begin{bmatrix} \sqrt{\gamma_1} & \sqrt{\gamma_2} \\ \sqrt{\gamma_1} & \sqrt{\gamma_2} \end{bmatrix}, \quad \boldsymbol{D} = i\boldsymbol{K} \tag{3}$$

where $\boldsymbol{a} = [a_1, a_2]^{\mathrm{T}}$, $\boldsymbol{s}^+ = \left[s_1^+, s_2^+\right]^{\mathrm{T}}$, and $\boldsymbol{s}^- = \left[s_1^-, s_2^-\right]^{\mathrm{T}}$. $\boldsymbol{H}$ is the Hamiltonian matrix of the coupled resonators, where $\omega_{1,2}$ and $\delta_{1,2}$ denote respectively the resonance frequency and damping factor of the resonators, $\gamma_{1,2}$ is the radiation loss, and κ is the coupling magnitude between two resonators.

We begin with the analysis of the system without air viscous damping, which means $\delta_{1,2} = 0$. The eigenvalues of the Hamiltonian $\boldsymbol{H}$ are given by [32]

$$\omega_{\pm} = \omega_{\mathrm{s}} + i\gamma_{\mathrm{s}} \pm \sqrt{(\omega_{\mathrm{c}} + i\gamma_{\mathrm{c}})^2 + \left(\kappa + i\sqrt{\gamma_1\gamma_2}\right)^2} \tag{4}$$

where $\omega_{\mathrm{s}} = (\omega_1+\omega_2)/2$, $\gamma_{\mathrm{s}} = (\gamma_1+\gamma_2)/2$, $\omega_{\mathrm{c}} = (\omega_1-\omega_2)/2$, and $\gamma_{\mathrm{c}} = (\gamma_1-\gamma_2)/2$. The bound state with zero radiation loss corresponds to a purely real eigenvalue, which is achieved when the following condition is satisfied [32]

$$\kappa(\gamma_1 - \gamma_2) = \sqrt{\gamma_1\gamma_2}(\omega_1 - \omega_2) \tag{5}$$

In this case, the eigenvalues reduce to

$$\begin{cases} \omega_{+} = \omega_{\mathrm{s}} + \frac{\kappa\gamma_{\mathrm{s}}}{\sqrt{\gamma_1\gamma_2}} + i(\gamma_1 + \gamma_2) \\ \omega_{-} = \omega_{\mathrm{s}} - \frac{\kappa\gamma_{\mathrm{s}}}{\sqrt{\gamma_1\gamma_2}} \end{cases} \tag{6}$$

It is seen that the resonance of frequency ω_- is free from radiation loss, while the other resonance at ω_+ becomes more lossy. The quality factor of the low-loss mode ω_- is defined as $Q_{\mathrm{CMT}} = \mathrm{Re}(\omega_-)/(2\mathrm{Im}(\omega_-))$, and it can reach infinity in theory when the BIC condition (5) is satisfied.

Based on the coupled mode Eq. (1), the transmission coefficient of the model system can be calculated by $T = s_2^-/s_1^+$, which results in

$$T = \frac{(\omega - \omega_1)(\omega - \omega_2) - \kappa^2}{\det(\omega\mathbf{I} - \boldsymbol{H}_0)} \tag{7}$$

where $\boldsymbol{H}_0$ denotes the Hamiltonian in the lossless case ($\delta_{1,2} = 0$) of Eq. (2), and $\mathbf{I}$ is the identity matrix. Five

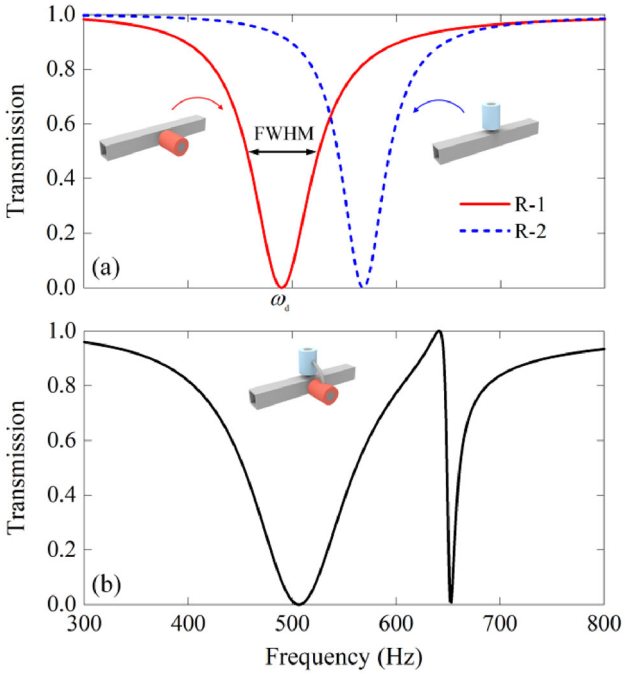

Fig. 2 Simulation results of the energy transmission spectrum of acoustic waveguide system connected to **a** a single resonator and **b** coupled resonators

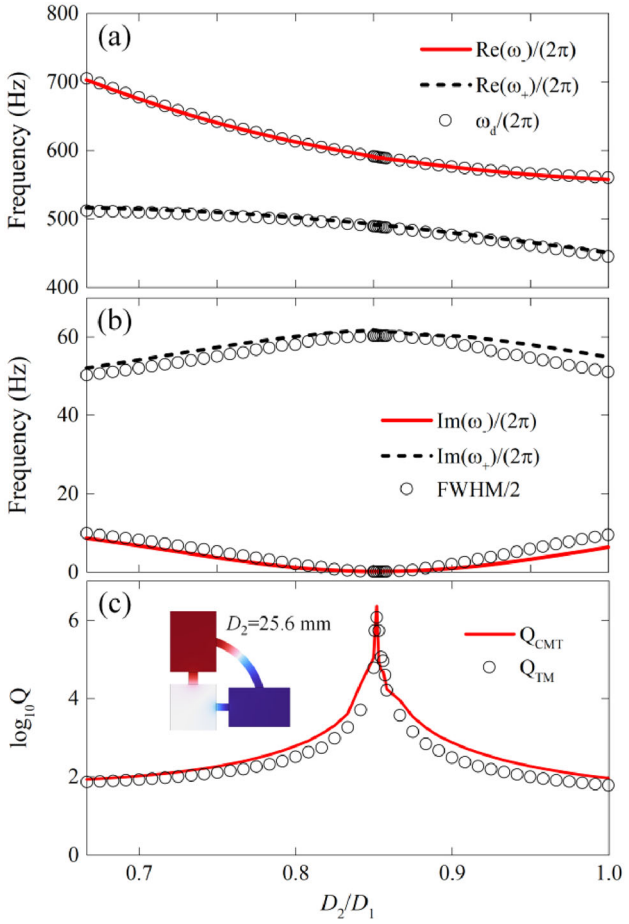

Fig. 3 **a** Real parts of $\omega_{\pm}$ and the dip transmission frequency ω_d as well as **b** imaginary parts of $\omega_{\pm}$ and the FWHM of transmission spectrum against the variation of D_2/D_1; **c** the quality factor of the low-loss resonance mode ω_-

Hamiltonian parameters ($\omega_{1,2}$, $\gamma_{1,2}$, and κ) can be identified by numerically calculating transmission spectra and fitting them with the results of Eq. (7), as detailed in the Supplementary Material [33]. According to this fitting method and BIC condition (5), the structural parameters of the coupled-resonator system with high-Q performance can be designed.

As an example, consider the geometric parameters: $L = 30$ mm, $d_1 = 6$ mm, $D_1 = 30$ mm, $d_2 = 5$ mm, $D_2 = 22$ mm, $l_{1(2)} = 8$ mm, $L_{1(2)} = 40$ mm, $d_c = 5.1$ mm, and $R_c = 45$ mm. The density $\rho_0 = 1.21$ kg/m^3 and sound velocity $c_0 = 343$ m/s are chosen for air. Figure 2a, b show the energy transmission spectra of the waveguide connected to a single resonator and to coupled resonators, respectively. The resonance results in a transmission drop, reaching a minimum at frequency ω_d. The radiation loss of this resonant state can be measured by the full width at half maximum (FWHM), with the quality factor defined as $Q_{TM} = \omega_d/\text{FWHM}$. It can be seen from Fig. 2b that the coupled resonance provides a means to redistribute the radiation loss in such a way that one resonance is modulated with a higher Q at the cost of increased loss in another. This is the key idea of the BIC to achieve high-Q performance.

To further disclose the underlying mechanism, the acoustic transmission of the coupled-resonator system with various D_2 is calculated. The dip transmission frequency ω_d and FWHM are retrieved, as shown in Fig. 3a, b, respectively. To verify the relationship between transmission behavior and the coupled-mode model, the Hamiltonian parameters $\omega_{1,2}$, $\gamma_{1,2}$, and κ are calculated via a fitting method and used to compute $\omega_{\pm}$ based on Eq. (4), as shown in Fig. 3a, b. The numerical simulation results align closely with Eq. (4), showing the approximate relationships of $\omega_d \approx \text{Re}(\omega_{\pm})$ and $\text{FWHM} \approx 2\text{Im}(\omega_{\pm})$. This also leads to the results of $Q_{TM} \approx Q_{CMT}$, as verified in Fig. 3c.

According to Fig. 3, a quasi-BIC can be achieved at $D_2 = 25.6$ mm with the quality factor approaching 10^6. The corresponding scattering pressure field of the system is shown in the inset of Fig. 3c. It is seen that the interference interaction of the two resonators results in the field distribution with a minor scattering from resonators to the waveguide, disclosing the nature of Friedrich-Wintgen BICs [22–26].

3 Gain-Assisted System with High-Q Performance

Figure 4(a) shows the transmission spectrum of the lossless quasi-BIC system with $D_2 = 25.6$ mm, where a sharp

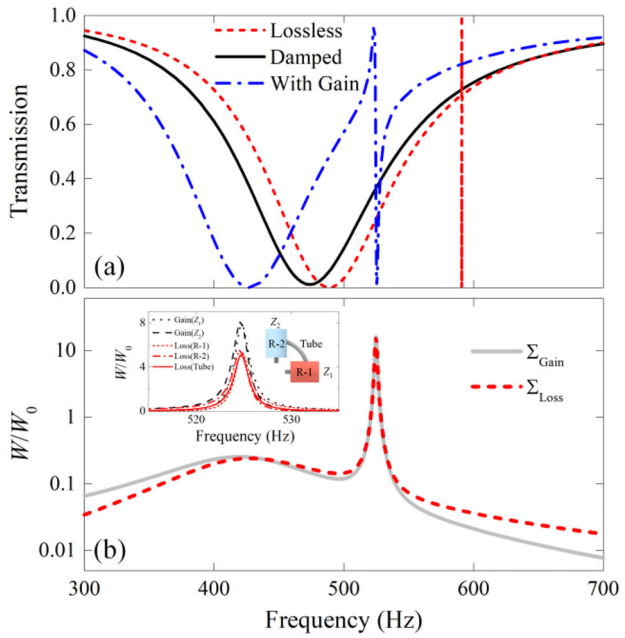

Fig. 4 **a** Simulation results of energy transmission spectra of a lossless quasi-BIC system, the same system but with intrinsic viscous damping, and that being added with the energy gain to compensate for intrinsic loss; **b** the net energy input $\sum_{gain}$ and dissipation $\sum_{loss}$ in gain-assisted systems, where the inset shows the energy distribution in sub-systems

resonance can be observed near the frequency of 591 Hz. However, this high-Q performance of acoustic quasi-BIC resonance disappears when there is air viscous damping in the system. Notice that the numerical simulation of damped systems is based on the thermal-viscous damping module of COMSOL Multiphysics [33]. In this section, the method to enhance the quality factor of damped systems is discussed by introducing acoustic gain effect.

In our model, acoustic gain is introduced by setting acoustic impedance conditions $Z_{1,2} = \rho_0 c_0 (R_{1,2} + \mathrm{i}X_{1,2})$ at the bottom edge of the resonator chamber, which occupies a circular area of diameters $D_{1,2}/2$, as sketched in Fig. 1. Energy can be pumped into the system by implementing negative acoustic resistance ($R_{1,2} < 0$), which is practically realizable through techniques of loudspeaker structures with shunting circuits [30, 34] or active feedback control systems [35, 36].

For damped systems with $\delta_{1,2} \neq 0$, the transmission coefficient can be calculated by the coupled mode Eq. (1), as given by

$$T = \frac{(\omega - \omega_1)(\omega - \omega_2) - \kappa^2 - \Delta}{\det(\omega \mathbf{I} - \boldsymbol{H})} \tag{8}$$

where $\boldsymbol{H}$ is given by Eq. (2), and

$$\Delta = i\delta_1(\omega - \omega_2) + i\delta_2(\omega - \omega_1) + \delta_1\delta_2 \tag{9}$$

For systems with air viscous damping and impedance boundary $Z_{1,2}$, seven Hamiltonian parameters ($\omega_{1,2}$, $\gamma_{1,2}$, $\delta_{1,2}$, and κ) are identified by fitting simulation results of transmission spectra with the results of Eq. (8) [33]. To achieve a high quality factor for damped systems, a necessary condition is to require $\delta_{1,2} = 0$, which is set to achieve the gain–loss balance such that the dissipated energy is exactly compensated by gain. As a result of the vanishing of the overall damping, the system operates in a lossless manner, and then the BIC condition (5) can be again used to achieve high-Q performance.

As an example, the damped system in Fig. 4a is added with impedance boundaries $X_1 = -5$ and $X_2 = -2.5$. According to the fitting method, acoustic resistances are determined as $R_1 = -1.178$ and $R_2 = -0.359$ such that the condition of $\delta_{1,2} = 0$ is fulfilled. The transmission spectrum of this gain-assisted system is plotted in Fig. 4a. The resonance behavior with a sharp transmission drop is recovered, showcasing a spectral profile similar to that of a lossless quasi-BIC system. To gain an insight into the gain–loss balance, we calculate the net power ($\sum_{loss}$) of energy dissipation due to viscous damping by two resonators and the coupling tube. In addition, the net power ($\sum_{gain}$) of energy input by gain in terms of impedance conditions Z_1 and Z_2 (at boundaries denoted by S) can be calculated by $W = 0.5\int_S \mathrm{Re}(p\, v_n^*)\mathrm{d}s$, where p and v_n refer to the pressure and normal velocity, respectively, and the symbol * denotes the complex conjugate. Figure 4b shows the net energy loss ($\sum_{loss}$) and gain ($\sum_{gain}$) normalized to acoustic power of incident waves, $W_0 = p_0^2 L^2/(2\rho_0 c_0)$, where p_0 is the wave amplitude, with the inset displaying the energy contributions by sub-systems. It is seen that the net energy loss and gain are exactly balanced near the resonance frequency of 525 Hz, as guaranteed by the condition of $\delta_{1,2} = 0$.

Acoustic reactance $X_{1,2}$ impacts the system by affecting Hamiltonian parameters $\omega_{1,2}$. For any sets of X_1 and X_2, R_1 and R_2 can be uniquely determined according to the gain–loss balance condition $\delta_{1,2} = 0$. Therefore, the BIC condition in gain-assisted systems can be fulfilled by tuning $X_{1,2}$. Based on the model of Fig. 4, we vary X_2 while keep other system parameters unchanged. Results of ω_d, FWHM, and $\omega_\pm$ against various X_2 are plotted in Fig. 5a, b in a similar style to Fig. 3a, b. Notice that the condition of $\delta_{1,2} = 0$ has been guaranteed for any case of X_2 by choosing proper $R_{1,2}$. Results confirm the relationship of $\omega_d \approx \mathrm{Re}(\omega_\pm)$ and $\mathrm{FWHM} \approx 2\mathrm{Im}(\omega_\pm)$. The resonance mode at ω_- can be modulated with a very low radiation loss at some specific X_2. Figure 5c shows the quality factors of this mode calculated by Q_{TM} and Q_{CMT}, which are in good agreement. A quasi-BIC can be found at $X_2 = -5$ with the quality factor up to 10^6, and the corresponding acoustic resistances are $R_1 = -1.126$ and $R_2 = -1.4$.

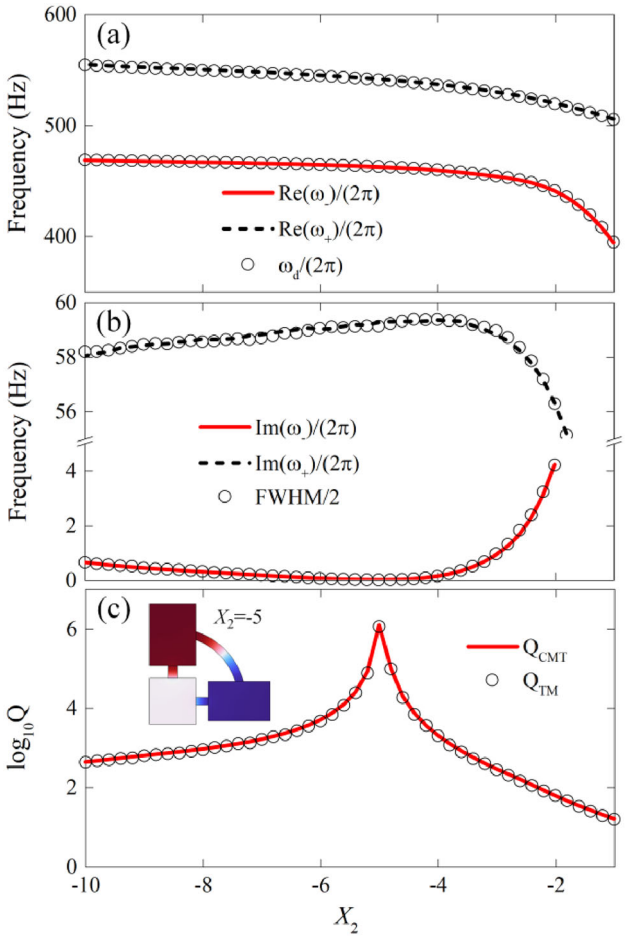

Fig. 5 **a–c** Results similar to Figs. 3a-c, but for gain-assisted systems

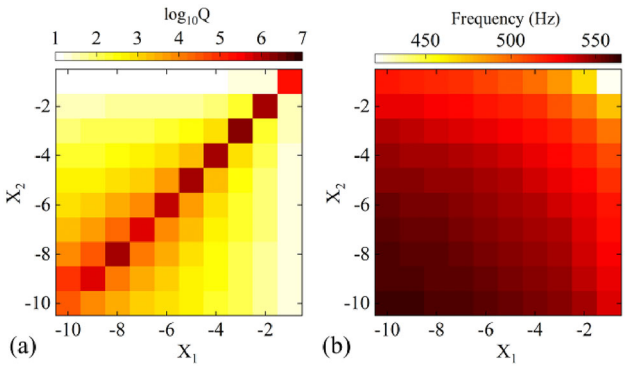

Fig. 6 **a** The quality factor Q_{TM} of gain-assisted resonance systems with various X_1 and X_2, and **b** the corresponding resonance frequencies

Modulation in the parameter space (X_1, X_2) would offer more possibilities to fulfill the high-Q condition (5). As an illustration, the quality factor Q_{TM} of the resonance is shown in Fig. 6a by varying both X_1 and X_2 for the model system of Fig. 4. Notice that the condition of $\delta_{1,2} = 0$ has been satisfied for any sets of X_1 and X_2 with proper choice of $R_{1,2}$. Results show that an extremely high Q can be achieved in systems with different sets of X_1 and X_2. The resonance with a high quality factor $Q > 10^6$ can appear at different frequencies occupying a finite bandwidth ranging from 493 to 555 Hz, as observed in Fig. 6b. This clearly demonstrates the design flexibility of X_1 and X_2 in manipulating the high-Q performance of acoustic quasi-BIC resonance and its corresponding frequency.

4 Sensor Model for Particle Size Detection

Based on the quasi-BIC concept in gain-assisted systems, we design a sensor model for particle size detection, and illustrate the superior sensing performance supported by the high-Q resonance. The schematic of the sensor model is shown in Fig. 7a. Acoustic energy transfer and interaction are significant in the waveguide region near the inlet ports of two Helmholtz resonators. In this region, the presence of scattering particles is expected to cause an obvious change in acoustic resonant response of incident waves, which can be used for sensing the presence of particles and detecting their volume sizes. To verify the sensing performance, an acoustically-rigid particle of a cubic block of length a is placed in the nearby region of two inlet ports. The particle size is characterized by its volume fraction with respect to the waveguide geometry, as defined by $\alpha = (a/L)^3$. The system parameters used in the sensor model are the same as those in Fig. 5a, b. $X_2 = -4.5$ is chosen to acquire the high-Q performance supported by a quasi-BIC, and a low-Q system is also introduced for comparison by setting $X_2 = -2.5$.

Figure 7b, c show the simulation results of transmission spectra for particles of different sizes ($\alpha = 0$, 3%, 6%, and 9%) in the high-Q ($X_2 = -4.5$) and low-Q ($X_2 = -2.5$) systems, respectively. It is clearly seen that the resonant frequency at which acoustic transmission significantly drops is shifted with the variation of the particle size. For further illustration, the shift of the resonant frequency for various particle sizes with respect to the empty case ($\alpha = 0$) is calculated, as shown in Fig. 7d. A nearly linear correlation can be observed, confirming that the model system can be used as a particle size sensor. The Q factors of resonances associated with different particle sizes are shown in Fig. 7e. They approach approximately 10^2 and 10^4 for the high-Q and low-Q systems, respectively. As a superior property, the sensor model is seen to possess a weak dependence of Q values on the size variation of particles under detection. Namely, a high quality factor, once designed in the absence of particles, can be maintained irrespective of particle size changes.

The sensor performance can be evaluated in terms of sensitivity and figure of merit (FoM). Here, sensitivity is defined as the resonant frequency shifting versus the particle size change, i.e., $S = \Delta f/\Delta\alpha$. According to Fig. 7d, the shift of

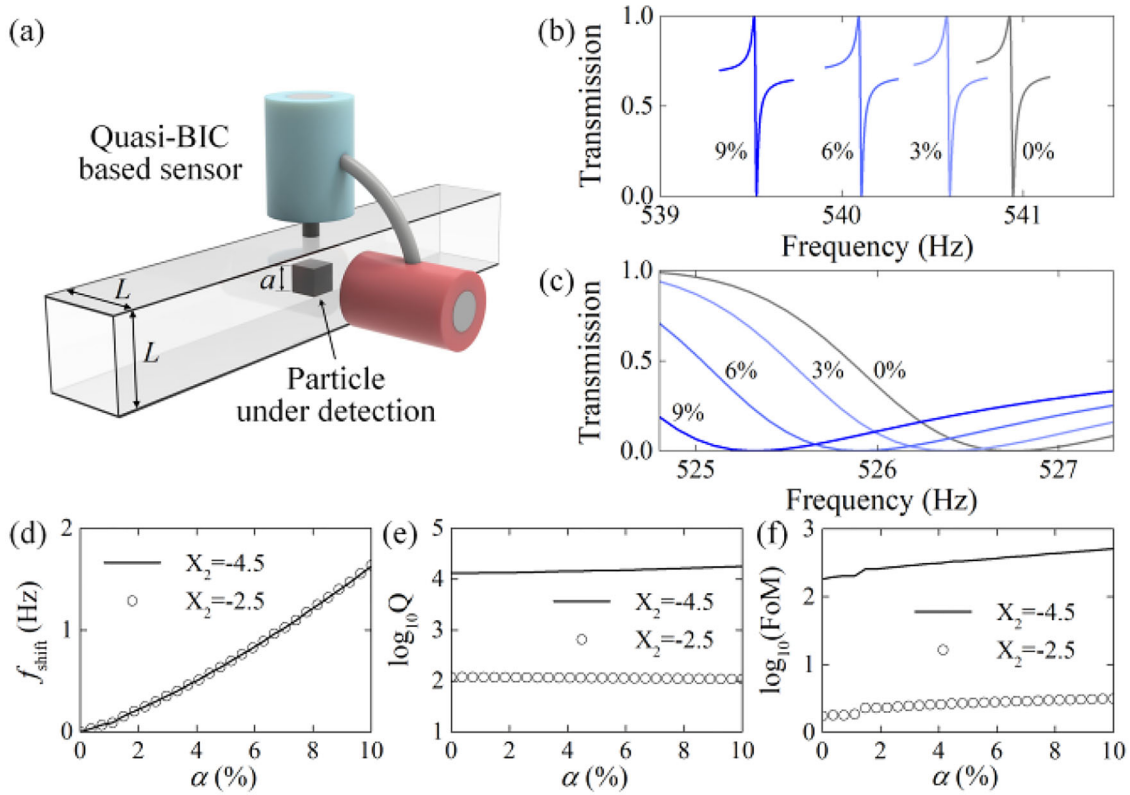

Fig. 7 **a** Schematic of the quasi-BIC-based sensor for particle size detection; simulation results of transmission spectra for particles of different sizes ($\alpha = 0$, 3%, 6%, and 9%) in the **b** high-Q ($X_2 = -4.5$) and **c** low-Q ($X_2 = -2.5$) systems; **d** the resonant frequency shifting with respect to the empty case ($\alpha = 0$), **e** the Q-factor, and **f** the FoM in the case of various particle sizes

resonant frequency against α coincides for high-Q and low-Q systems, which means the same sensitivity of the two systems. However, the FoM is related to both sensitivity and the Q factor, and is defined by FoM = S/FWHM. The FoM in the case of various particle sizes is shown in Fig. 7f. As a result of the quasi-BIC resonance, it is seen that the FoM of the high-Q system is two orders of magnitude greater than that of the low-Q system. This means that the quasi-BIC-based sensor with high FoM can more accurately detect the weak particle size variation.

5 Conclusion

The quality factor is an important parameter in sensing, filtering, and detection devices. In recent years, there has been increasing interest in achieving high-Q performance of resonance systems based on the bound states in the continuum. For a lossless system, the BIC condition is developed by pursuing a purely real eigenvalue of the system Hamiltonian. In a state close to the BIC, there is a minor radiation loss, which results in an extremely high quality factor. This work focuses on damped acoustic systems with intrinsic loss and presents a BIC-based method to enhance the quality factor by incorporating gain elements. The model system is a two-port acoustic waveguide connected to two directly coupled Helmholtz resonators. The dynamic equation for the coupled-resonator system is established based on the temporal coupled-mode theory, where the system Hamiltonian involves both intrinsic and radiation losses. To achieve high-Q performance in damped systems, acoustic gain is designed to exactly balance the intrinsic loss such that the damping factor of the system Hamiltonian vanishes. Meanwhile, the system parameters approach a quasi-BIC condition such that the radiation loss can be greatly suppressed. As a result of the reduction of both intrinsic and radiation losses, an extremely high quality factor can be achieved in gain-assisted acoustic resonance systems, as demonstrated by numerical simulations. It is worth noting that acoustic impedance boundary that produces the gain effect can offer more possibilities to fulfill the high-Q condition at different frequencies. Finally, a sensor model for particle size detection is proposed based on the gain-assisted system with quasi-BICs. The good sensing performance with high FoM is illustrated to demonstrate

the advantages of the studied high-Q acoustic system. The proposed method can be used to achieve high quality factors in acoustic systems with nontrivial intrinsic damping and improve the sensing performance of acoustic sensors and detection devices.

Supplementary Information The online version contains supplementary material available at https://doi.org/10.1007/s10338-024-00530-3.

Author Contributions LZ and XZ conceived the concept and model. LZ carried out the theoretical analyses and numerical simulations. XZ supervised the research. All authors discussed the results and wrote the manuscript.

Funding This work was supported by the National Natural Science Foundation of China (Grant Nos. 12225203, 11622215, and 11872111) and the 111 Project (Grant No. B16003).

Data Availability The data that support the findings of this study are available from the corresponding author upon reasonable request.

Declarations

Conflict of interests The authors declare that they have no competing interests.

References

1. Zhang JJ, Ruan YH, Hu ZD, Wu JJ, Wang JC. An enhanced high Q-factor resonance of quasi-bound states in the continuum with all-dielectric metasurface based on multilayer film structures. IEEE Sens J. 2023;23(3):2070–5.
2. Maksimov DN, Gerasimov VS, Romano S, Polyutov SP. Refractive index sensing with optical bound states in the continuum. Opt Express. 2020;28(26):38907–16.
3. Yin W, Shen ZL, Li SN, Cui YQ, Gao F, Hao HB, et al. THz absorbers with an ultrahigh Q-factor empowered by the quasi-bound states in the continuum for sensing application. Opt Express. 2022;30(18):32162–73.
4. Wang YL, Han ZH, Du Y, Qin JY. Ultrasensitive terahertz sensing with high-toroidal dipole resonance governed by bound states in the continuum in all-dielectric metasurface. Nanophotonics. 2021;10(4):1295–307.
5. Doskolovich LL, Bezus EA, Bykov DA. Integrated flat-top reflection filters operating near bound states in the continuum. Photon Res. 2019;7(11):1314–22.
6. Foley JM, Young SM, Phillips JD. Symmetry-protected mode coupling near normal incidence for narrow-band transmission filtering in a dielectric grating. Phys Rev B. 2014;89(16):165111.
7. Yesilkoy F, Arvelo ER, Jahani Y, Liu MK, Tittl A, Cevher V, et al. Ultrasensitive hyperspectral imaging and biodetection enabled by dielectric metasurfaces. Nat Photonics. 2019;13(6):390–6.
8. Wei JX, Chen Y, Li Y, Li W, Xie JS, Lee C, et al. Geometric filterless photodetectors for mid-infrared spin light. Nat Photon. 2023;17(2):171–8.
9. Huang LJ, Xu L, Woolley M, Miroshnichenko AE. Trends in quantum nanophotonics. Adv Quantum Technol. 2020;3(4):1900126.
10. Sadreev AF. Interference traps waves in an open system: bound states in the continuum. Rep Prog Phys. 2021;84(5):055901.
11. Song QJ, Dai SW, Han DZ, Zhang ZQ, Chan CT, Zi J. PT symmetry induced rings of lasing threshold modes embedded with discrete bound states in the continuum. Chin Phys Lett. 2021;38(8):084203.
12. Huang LJ, Xu L, Powell DA, Padilla WJ, Miroshnichenko AE. Resonant leaky modes in all-dielectric metasystems: fundamentals and applications. Phys Reports-Rev Sect Phys Lett. 2023;1008:1–66.
13. Pappademos J, Sukhatme U, Pagnamenta A. Bound-states in the continuum from supersymmetric quantum-mechanics. Phys Rev A. 1993;48(5):3525–31.
14. Cong LQ, Singh R. Symmetry-protected dual bound states in the continuum in metamaterials. Adv Optical Mater. 2019;7(13):1900383.
15. Huang LJ, Chiang YK, Huang SB, Shen C, Deng F, Cheng Y, et al. Sound trapping in an open resonator. Nat Commun. 2021;12(1):4819.
16. Koshelev K, Bogdanov A, Kivshar Y. Meta-optics and bound states in the continuum. Sci Bull. 2019;64(12):836–42.
17. Sidorenko MS, Sergaeva ON, Sadrieva ZF, Roques-Carmes C, Muraev PS, Maksimov DN, et al. Observation of an accidental bound state in the continuum in a chain of dielectric disks. Phys Rev Appl. 2021;15(3):034041.
18. Huang LJ, Jia B, Pilipchuk AS, Chiang YK, Huang SB, Li JF, et al. General framework of bound states in the continuum in an open acoustic resonator. Phys Rev Appl. 2022;18(5):054021.
19. Sadrieva ZF, Sinev IS, Koshelev KL, Samusev A, Iorsh IV, Takayama O, et al. Transition from optical bound states in the continuum to leaky resonances: role of substrate and roughness. ACS Photon. 2017;4(4):723–7.
20. Marinica DC, Borisov AG, Shabanov SV. Bound states in the continuum in photonics. Phys Rev Lett. 2008;100(18):183902.
21. Huang L, Jia B, Chiang YK, Huang S, Shen C, Deng F, et al. Topological supercavity resonances in the finite system. Adv Sci. 2022;9(20):2200257.
22. Lyapina AA, Maksimov DN, Pilipchuk AS, Sadreev AF. Bound states in the continuum in open acoustic resonators. J Fluid Mech. 2015;780:370–87.
23. Azzam SI, Shalaev VM, Boltasseva A, Kildishev AV. Formation of bound states in the continuum in hybrid plasmonic-photonic systems. Phys Rev Lett. 2018;121(25):253901.
24. Pilipchuk AS, Pilipchuk AA, Sadreev AF. Bound states in the continuum in open spherical resonator. Phys Scr. 2020;95(8):085002.
25. Huang SB, Liu T, Zhou Z, Wang X, Zhu J, Li Y. Extreme sound confinement from quasibound states in the continuum. Phys Rev Appl. 2020;14(2):021001.
26. Liu SS, Huang SB, Zhou ZL, Qian P, Jia B, Ding H, et al. Observation of acoustic Friedrich-Wintgen bound state in the continuum with bridging near-field coupling. Phys Rev Appl. 2023;20(4):044075.
27. Gu ZM, Gao H, Cao PC, Liu T, Zhu XF, Zhu J. Controlling sound in non-hermitian acoustic systems. Phys Rev Appl. 2021;16(5):057001.
28. Ding K, Fang C, Ma GC. Non-Hermitian topology and exceptional-point geometries. Nat Rev Phys. 2022;4(12):745–60.
29. Huang LJ, Huang SB, Shen C, Yves S, Pilipchuk AS, Ni X, et al. Acoustic resonances in non-Hermitian open systems. Nat Rev Phys. 2024;6(1):11–27.
30. Fleury R, Sounas D, Alù A. An invisible acoustic sensor based on parity-time symmetry. Nat Commun. 2015;6(1):5905.
31. Suh W, Wang Z, Fan SH. Temporal coupled-mode theory and the presence of non-orthogonal modes in lossless multimode cavities. IEEE J Quantum Electron. 2004;40(10):1511–8.
32. Hsu CW, Zhen B, Stone AD, Joannopoulos JD, Soljacic M. Bound states in the continuum. Nat Rev Mater. 2016;1(9):1–13.
33. See supplemental material for details of the fitting method and simulation model
34. Huang Y, Zhou XM. Non-reciprocal sound transmission in electro-acoustic systems with time-modulated circuits. Acta Mech Solida Sin. 2022;35(6):940–8.

35. Geib N, Sasmal A, Wang ZZ, Zhai YX, Popa BI, Grosh K. Tunable nonlocal purely active nonreciprocal acoustic media. Phys Rev B. 2021;103(16):165427.
36. Cheng W, Hu GK. Odd elasticity realized by piezoelectric material with linear feedback. Sci Chin-Phys Mech Astron. 2021;64(11):2.
37. Li DT, Huang SB, Cheng Y, Li Y. Compact asymmetric sound absorber at the exceptional point. Sci Chin-Phys Mech Astron. 2021;64(4):244303.